Biosensors and Bioelectronics 126 (2019) 324–331

Contents lists available at ScienceDirect

Biosensors and Bioelectronics

journal homepage: www.elsevier.com/locate/bios

Plasmonic enhancement in lateral flow sensors for improved sensing of *E. coli* O157:H7

Wen Ren[a], Dexter R. Ballou[b], Ryan FitzGerald[c], Joseph Irudayaraj[c,*]

[a] Department of Agricultural and Biological Engineering, Bindley Bioscience Center, Purdue University, 225 South University Street, West Lafayette, IN 47907, US
[b] Department of Materials Science and Engineering, University of Illinois at Urbana and Champaign, 1304 W Green St, Urbana, IL 61801, US
[c] Department of Bioengineering, University of Illinois at Urbana and Champaign, 208 North Wright Street, Urbana, Illinois 61801, US

ARTICLE INFO

Keywords:
Lateral flow sensor
E. coli O157:H7
Plasmonic enhancement
Liposome
Gold nanoparticle aggregation, rapid detection

ABSTRACT

We propose a plasmonic enhanced lateral flow sensor (pLFS) concept with an enhanced colorimetric signal by utilizing liposome encapsulating reagent to trigger the aggregation of gold nanoparticles (GNPs). Our signal enhancement strategy incorporates the simplicity of lateral flow immunoassays (LFIA) utilizing plasmonic enhancement. The conceptualized hybrid pLFS for onsite rapid detection of pathogens in low numbers in a user friendly format requiring simple steps is the first step in the translation of plasmonic enhancement sensing to a practical regime. The pLFS was carried out with a biotinylated liposome label ruptured to release branched polyethylenimine (BPEI) to trigger the aggregation of GNPs for colorimetric signal generation. BPEI has multiple amino groups and more positive charges in PBS buffer, therefore few of the BPEI groups could induce the aggregation of GNPs, resulting in an enhanced colorimetric signal to detect *E. coli* O157:H7. Compared with the reported conventional LFIA, the proposed pLFS demonstrated more than 1000-fold improvement in sensitivity. The pLFS could detect as low as 100 CFU/ml of *E. coli* O157:H7 in buffer and 600 CFU/ml *E. coli* O157:H7 in liquid food systems.

1. Introduction

Lateral flow immunoassay (LFIA) has held its place as a very practical analytical method for the detection and evaluation of various targets including nucleic acids, protein, and whole organisms such as virus and bacteria because of its simplicity and onsite usability (Cho and Irudayaraj, 2013b; Corstjens et al., 2003; Liu et al., 2006; Mao et al., 2009; Ren et al., 2016). LFIA has been used in food safety and public health screening including clinical diagnosis for point-of-care testing and in-situ monitoring. LFIA systems based on fluorescence or other spectral analysis require instrumentation for signal readout (Gumustas et al., 2018; Hua et al., 2015; Li et al., 2010; Luo et al., 2017; Rajendran et al., 2014; Song et al., 2016; Xing et al., 2018; Xu et al., 2009), while colorimetric signals are easier to use because of the direct inspection of results with naked eyes. Signals from colorimetry are usually weak hence sensitive detection is not possible. To improve the sensitivity of colorimetric LFIA several prior work exists with polymer nanoparticles or latex beads loaded with color inducing chemicals (Cox et al., 2015; Imamura et al., 2015; Lee et al., 2016) while metal nanoparticles are still commonly used as substrates for LFIA probes. Metal nanoparticles, due to its plasmonic feature, usually has large extinction coefficient, and thus a small amount of nanoparticles could provide a visible color (Doremus, 1964; Guo and Wang, 2011). Among metal nanoparticles, gold nanoparticles (GNPs) have been widely used in LFIA colorimetry because of its stability and biocompatibility. In spite of the large extinction coefficient detecting at low target levels with GNPs induced colorimetry is still a challenge since the color generated from the probes anchored at the detection zone is very weak. The sensitivity possible for whole cell detection with conventional LFIA was around 10^5–10^6 CFU/ml (Pengsuk et al., 2013; Preechakasedkit et al., 2012), which is not sufficient for effective food safety monitoring. Hence, enhancement of the colorimetric signal is critical for LFIA applications.

Silver enhancement enabled by reducing the silver substrate solution to metallic silver structures around the probes in the detection zone due to target capture has been proposed (Panferov et al., 2016; Shin et al., 2018; Wiederoder et al., 2017). The generated silver structures could provide stronger visible signals, however nonspecific reduction limits the application of silver enhancement in LFIA systems (Linares et al., 2012). Enzyme based colorimetric signal amplification was suggested to provide higher enhancement. When enzymes are conjugated to the probes, the presence of targets was represented by the color generated from the enzyme-catalyzed reaction products. In our

* Corresponding author.
E-mail address: jirudaya@illinois.edu (J. Irudayaraj).

https://doi.org/10.1016/j.bios.2018.10.066
Received 12 August 2018; Received in revised form 18 October 2018; Accepted 30 October 2018
Available online 01 November 2018
0956-5663/

Table 1
Detection performance of pLFS compared to LF-based methods for whole bacteria.

	Sensitivity (CFU/ml)	Detection time (min)	Signal
pLFS	100	~45	GNP aggregates
Conventional LFIA (Pengsuk et al., 2013; Preechakasedkit et al., 2012)	10^4–10^5	~10	GNP probes
LFIA with hierarchical GNPs (Zhang et al., 2015)	10^3	~15	Tipped flowerlike GNPs
Enzyme enhanced LFIA (Cho and Irudayaraj, 2013b)	100	~25	Colorimetric product of enzymatic reaction
Magnetic focus enhanced LFIA (Ren et al., 2016)	25	~45	Colorimetric product of enzymatic reaction

previous work, we have shown that an enzyme enhanced LFIA with GNP probes immobilized with horseradish peroxidase (HRP) can be used for bacteria detection (Cho and Irudayaraj, 2013b). After the flow of sample along the LF strip, the strip was washed, and 3,3′,5,5′-tetramethylbenzidine (TMB) was added by cross flow. The obtained green color due to the HRP-catalyzed TMB reaction represents the target bacteria and a limit of detection down to 100 CFU/ml was possible. Assisted by magnetic focus, a sensitivity as low as 25 CFU/ml in PBS buffer was possible (Ren et al., 2016). However, it should be noted that the enzyme catalyzed reaction could be influenced by the detection environment and the presence of non-targets in real samples contributing to nonspecific signals, while the stability of bioactive enzyme modified probes would limit the application. Thus, a non-reaction based enhancement strategy for colorimetric LFIA could further advance this technology.

A strategy for plasmonic enhancement of colorimetric signals in enzyme-linked immunosorbent assays (ELISA), termed as plasmonic ELISA was proposed. In plasmonic ELISA, enzyme was still necessary to consume the added H_2O_2, whose concentration determined the generation and aggregation of GNPs along with the color from being colorless to red or even blue as the colorimetric signal (De La Rica and Stevens, 2012, 2013; Gobbo et al., 2013). Instead of H_2O_2, in plasmonic ELISA acetylthiocholine was used which could be hydrolyzed by acetylcholinesterase.(Nie et al., 2014). The thiochioline produced could trigger the aggregation of as-prepared GNPs to generate the color change from red to blue for colorimetric detection. However, the use of enzyme still limits the application of these plasmonic ELISA methods. Based on the concept of color change due to the aggregation of GNPs, Abbas et al. proposed a liposome based plasmonic ELISA method (Bui et al., 2015), where liposomes loaded with L-cysteine was used to label the target. The labeled liposome was then ruptured with Tween-20 in PBS and the released L-cysteine triggered the aggregation of the added GNPs for colorimetric determination of target bacteria. The liposome-amplified plasmonic ELISA did not require an enzymatic reaction. Besides, the possibility of loading the liposomes with different chemicals for colorimetric signal generation suggests a promising colorimetric enhancement strategy.

Irrespective of the detailed differences in detection steps, LFIA and ELISA have a similar recognition pattern and requires sample to be present in the liquid format (Cho and Irudayaraj, 2013a; Pappert et al., 2010). Therefore, an enhancement strategy for colorimetric ELISA could be potentially utilized for a LF platform. Compared with ELISA, LFIA detection is rapid in simple protocol. Herein, we propose a plasmonic enhanced lateral flow sensor (pLFS) concept by introducing a liposome-based amplification of the colorimetric signals on the lateral flow platform for ultrasensitive detection of pathogens. In pLFS, liposomes loaded with chemicals were anchored at the detection zone in the presence of targets. The liposomes are ruptured to release the chemical to trigger the aggregation of GNPs. The resulting aggregates of GNPs were trapped in the framework of nitrocellulose membrane after washing to form red spots. In the absence of target no liposomes were present in the detection zone and no aggregation occurred, hence the added GNP monomers were washed away and did not give rise to any color on the LF strip. Thus, the colorimetric signal from the trapped aggregates of GNPs could determine the target captured. Instead of L-cysteine, branched polyethylenimine (BPEI) was loaded in the liposomes to facilitate the cross-linking and aggregation of GNPs due to the amino groups. Compared to the signals from conventional LFIA systems with GNPs themselves, a stronger colorimetric signals in pLFS originated from the trapped GNP aggregates, to result in better sensitivity. Since enzymes were not required, the deviation of enzyme activity and non-specific interaction in the pLFS can be avoided.

To demonstrate the detection performance of the pLFS concept proposed in this work, *E. coli* O157:H7 was chosen as the target. It is known as the Shiga toxin-producing pathogen could induce various diseases to result in up to 40% mortality and thus is a serious threat to food safety and public health (Chen and Frankel, 2005; Famewo et al., 2016; Ren et al., 2018). The proposed pLFS could recognize as low as 100 CFU/ml of *E. coli* O157:H7 within 45 min, which is over 1000 times more sensitive than the sensitivity possible by conventional LFIA (10^5–10^6). The detection time by pLFS was much shorter than ELISA which requires 3–4 h. Compared with the reported detection method for *E. coli* O157:H7 which is based on the plasmon shift of SiO_2 coated gold nanorods and requires a signal readout with instrumentation (Song et al., 2017), pLFS can detect 100 CFU/ml of the pathogens with naked eyes due to the formation of red spots on LF strips. The capability of pLFS was also demonstrated in liquid food such as cranberry juice, and a recognition of 600 CFU/ml of *E. coli* O157:H7 was possible. Table 1 was provided to further demonstrate the detection performance of pLFS referring to some LF-based detection platforms. The developed plasmonic enhancement strategy is unique and versatile for rapid onsite detection.

2. Experimental section

2.1. Materials

$HAuCl_4{\cdot}3H_2O$, sodium citrate dihydrate, Na_2CO_3, BPEI (Mn = ~1800) and cholesterol were purchased from Sigma-Aldrich (St. Louis, MO). *L*-α-phosphotidylcholine (PC) and phosphoethanolamine-conjugated biotin (DSPE-PEG2000-biotin) were obtained from Avanti Polar Lipids (Alabaster, AL). Sulfo-NHS-LC-biotin was purchased from Thermal Scientific (Rockford, IL). Polyclonal antibody against *E. coli* O157:H7 (01-95-90) and heat-treated *E. coli* O157:H7 for positive control were acquired from KPL (Gaithersburg, MD). All chemicals were used as received. All glasswares were cleansed with fresh aqua regia and rinsed with DI water.

2.2. Preparation of GNPs and GNP probes

GNPs used for pLFS were synthesized based on the reported method (Frens, 1973). Briefly, 1 ml of 1% $HAuCl_4{\cdot}3H_2O$ was added to 100 ml of boiling DI water. To the obtained 18 nm GNPs, under strong stirring, 1 ml of 1% sodium citrated was added and the solution was kept at boiling for an additional 15 min. For 40 nm GNPs, 0.5 ml of 1% sodium citrate was added. The obtained GNPs were cooled down to room temperature and kept at 4 °C for subsequent experiments. The size and concentration was calculated with the method reported by Haiss et al. (2007) based on the UV–vis spectra collected with a Genesystm 10S UV–vis Spectrophotometer.

GNP probes were fabricated based on our previous method with modification (Cho and Irudayaraj, 2013b; Ren et al., 2016; Ren et al.,

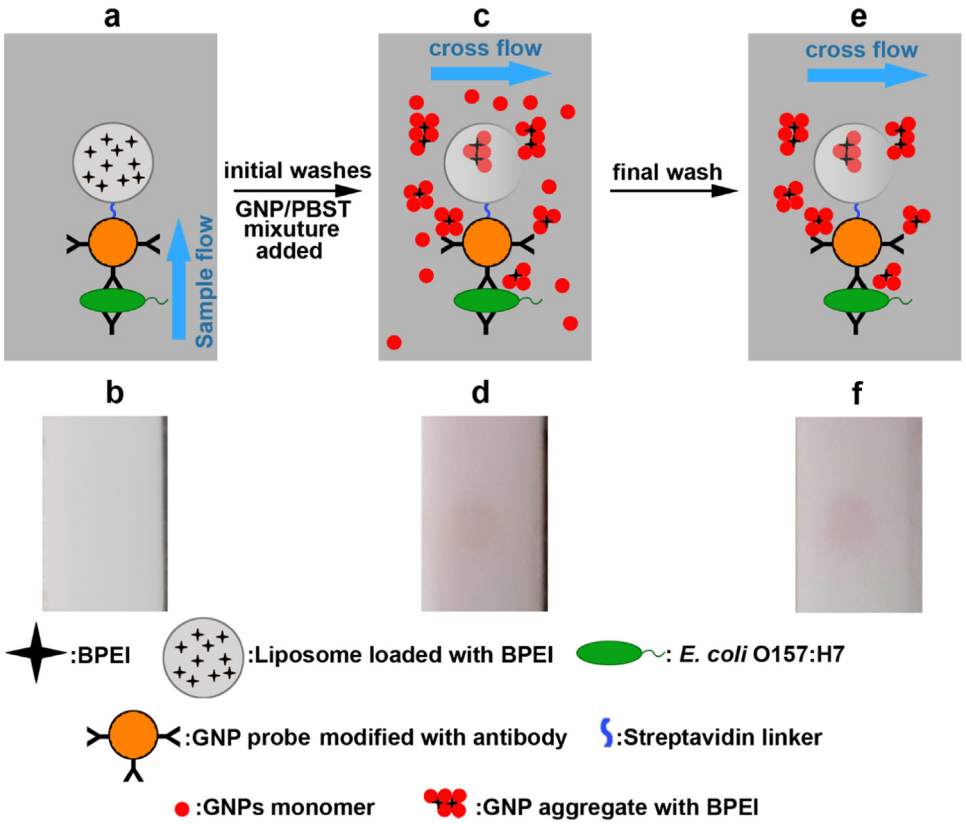

Scheme 1. Colorimetric signal generation process in pLFS.

2017). Briefly, 500 µl of 40 nm GNPs were added with 50 µl of 10 mM PB buffer, followed by the addition of 1 µl of 0.5 M Na_2CO_3. After mixing well, 5 µl of 1 mg/ml polyclonal antibody against *E. coli* O157:H7 was injected. The obtained solution was shaken for 4 h at room temperature. Then 55 µl of 5% casein in 10 mM PB buffer was added and shaken for 1 h to block the unreacted surface. The obtained GNPs was centrifuged at 8000 rpm for 10 min and washed with 10 mM PB buffer two times. After redispersing in 500 µl of 10 mM PB buffer, the antibody modified GNPs were biotinylated by the addition of 10 µg sulfo-NHS-LC-biotin and the solution was shaken at room temperature for 1 h. The resulting GNP probes were washed with 10 mM PBS buffer two times and redispersed in 500 µl of 10 mM PBS.

2.3. Synthesis of BPEI-loaded liposome

The synthesis of liposomes loaded with BPEI was performed based on published methods with slight modification (Bui et al., 2015; Gomes et al., 2006). In a reserve-phase evaporation process, 140 µl of 5 mg/ml PC in chloroform was added with 20 µl of 5 mg/ml cholesterol in chloroform and 40 µl of 5 mg/ml DSPE-PEG2000-biotin in chloroform in a glass vial. After rotation for the formation of a uniform layer of the solution, the glass vial was vacuumed overnight to evaporate the chloroform. To the glass vial, 1 ml of 100 µg/ml BPEI was added and the solution was vortexed for 2 min to result in the formation of cloud-like multilamellar liposomes. The prepared liposomes were purified by dialysis with a dialysis membrane (MWCO 14 kDa, Spectrum, Inc., Rancho Dominguez, CA) and the size of the obtained liposome was determined to be 172.6 ± 6.5 nm with a dynamic light scattering particle size analyzer (Malvern Zetasizer ZS90). The concentration of liposome was estimated to be around 1.73×10^{11} liposome/ml based on the procedure described by Abbas et al (Bui et al., 2015).

2.4. Plasmonic enhanced lateral flow sensor development

Lateral flow strips were assembled on a plastic backboard, on which 2.5 cm length of nitrocellulose membrane was fixed at a position of 1.3 cm from one end of the strip. An absorbent pad 1.5 cm in length was fixed at the end of the strip, while at the other end of the nitrocellulose membrane, a 1.1 cm of conjugate pad and 1.7 cm of sample pad was assembled on the plastic backboard. Each part had a 0.2 cm overlap area to ensure continuity in sample flow. The width of the strip was set at 0.5 cm. On the prepared LF strip, 0.9 µl of 0.33 mg/ml of polyclonal antibody against *E. coli* O157:H7 was dropped on the nitrocellulose membrane and the strip was dried at 37 °C for 1 h.

The detection process with pLFS is illustrated in Fig. S1. To detect bacteria, 100 µl of sample solution containing serial concentration of *E. coli* O157:H7 was added with 5 µl of GNP probes and 0.5 µl of 1 mg/ml streptavidin. Then the sample was incubated at room temperature for 10 min, followed by the addition of 5 µl of BPEI-loaded liposomes. After 5 min of incubation, the sample solution was loaded on the sample pad of the lateral flow strip for 10 min of sample flow. A conjugate pad and an absorbent pad at 1.1 cm × 1.3 cm were fixed at both sides of the strip respectively and 60 µl of DI water was added to the conjugate pad to wash the detection zone twice at 5 min interval. Then 60 µl of GNPs in PBST (1:2 ratio, PBST: 0.5% tween-20 in 10 mM PBS) was added for colorimetric signal generation. After 5 min, 60 µl of DI water was applied for one more wash and the results were recorded with a camera.

Cranberry juice was obtained from a local grocery store and its pH was adjusted with 1 M NaOH. To reduce the influence from thickening agents the juice was diluted with 10 mM PBS at 1:1 ratio. Known concentration of *E. coli* O157:H7 was purposefully inoculated into the juice sample and the resulting solution was used as a food sample in the pLFS.

All experiments were replicated 3 times. To quantify the colorimetric signals, images of the strips were recorded after detection. The

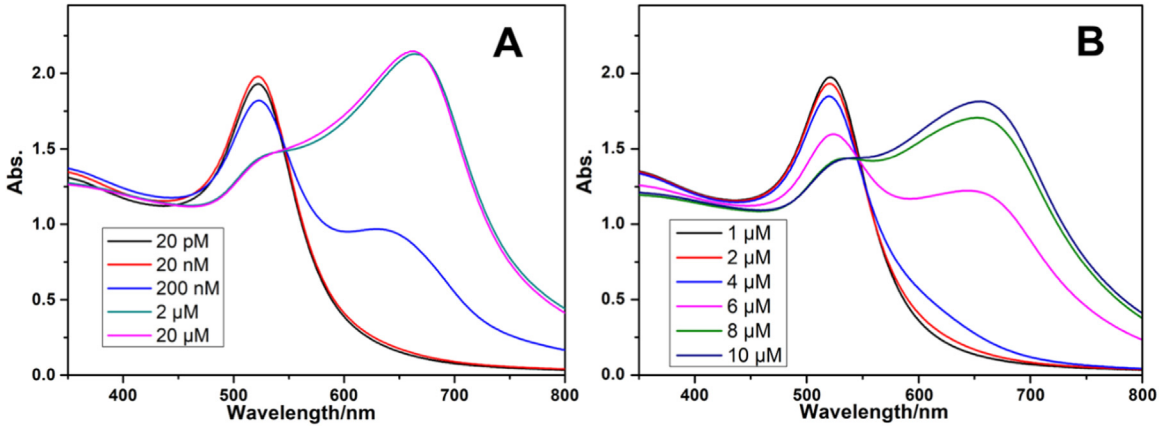

Fig. 1. The UV-spectra of 18 nm GNPs with serial concentration of BPEI (A) and L-cysteine (B).

brightness and contrast of the images was adjusted and converted to monochrome format. Then ImageJ was used to measure the gray scale value of the dots from the GNP aggregates and the blank area around the dots. The difference between the gray scale value from dots and corresponding blank area was used for quantification.

3. Results and discussion

The plasmonic enhancement concept implemented in a lateral flow devise utilizing liposomes encompass the advantages of plasmonic ELISA while retaining the merits of a lateral flow devise. The plasmonic enhancement strategy of pLFS is illustrated in Scheme 1. The target *E. coli* O157:H7 is first labeled with GNP probes which comprise of gold nanoparticles modified with antibody and biotinylated. The BPEI-loaded liposome particles were then linked to GNP probes through streptavidin-biotin linkage. In the sample flow along the strip, as shown in Scheme 1a, the labeled *E. coli* O157:H7 is captured by antibodies immobilized on the LF strip to form a structure comprising of antibody on strip/captured target bacterium/labeled GNP probe/linked liposome loaded with BPEI. It can be seen in Scheme 1b that there was no visible color on the LF strip, suggesting that the limited number of GNP probes conjugated to the LF strip due to the low concentration of target bacteria will not generate any signal. After two initial washes via cross flow, the GNPs/PBST mixture was added on the strip as shown in Scheme 1c. PBST will rupture the liposomes and release the BPEI. The released BPEI will cross-link with the added GNPs to initiate its aggregation. The obtained aggregates were distributed in the detection zone where the liposomes were anchored, represented by the red spot in Scheme 1d. The color change from red to blue due to aggregation of GNPs was also not observed on the LF strip, which may be attributed to the limited space in the nitrocellulose membrane where the amount of added GNPs was not sufficient to form larger aggregates to cause the color change. At the final washing step, GNP monomers were removed along with the washing solution. In contrast, aggregates of GNPs due to the presence of BPEI were retained in the detection zone since the aggregates were larger in size compared to the GNP monomers and could not be removed from the LF strip with the washing solution. It should be noted that the GNPs at the sites away from the red dots did not aggregate because the amount of BPEI released was not sufficient to induce aggregation and thus were removed in the last wash step. Scheme 1f shows that the red spot remained in the detection zone while the rest of the region on the strip was cleaner than that shown in Scheme 1d, providing evidence that after the final wash the aggregates of GNPs linked by BPEI were retained in the nitrocellulose membrane and the GNP monomers were removed. Images shown as Scheme 1b, d, f reveals the detection mechanism of the developed pLFS: without target bacteria, no liposome was retained in the detection zone after initial washing steps, thus GNPs present in the monomer form were washed away in the final wash; in the presence of target bacteria the BPEI-loaded liposome would be anchored in the detection zone through the labeled probe, where the released BPEI could cross-link the added GNPs to form aggregates which remained in nitrocellulose membrane after washing to result in visible red dots. An increase in the concentration of target bacteria would link more liposomes and the corresponding increase in BPEI released could contribute to the formation of more aggregates to result in higher intensity of red dots in the detection zone.

As illustrated in Scheme 1, the colorimetric signal for the determination of bacteria concentration is due to the aggregation of added GNPs triggered by the chemicals released. It can therefore be expected that utilizing chemicals which could induce the aggregation at lower concentration a better detection sensitivity could be achieved. In previous reported efforts, L-cysteine was used to trigger the aggregation for the plasmonic enhancement (Bui et al., 2015). Considering the molecular size and amino group present, it is believed that polymer like BPEI with multiple amino groups could induce the aggregation at lower concentration compared to that with L-cysteine resulting in an improved sensitivity. To compare the aggregation behavior of GNPs with BPEI or L-cysteine, UV–vis spectra of GNPs were recorded with BPEI or L-cysteine at serial concentration in PBST and the spectra were shown in Fig. 1. The increased UV absorbance at longer wavelength range indicates the aggregation of GNPs. It can be seen that a significant aggregation of 18 nm GNPs occurred at 200 nM BPEI concentration while to observe the aggregation of GNPs ~4 μM or more of L-cysteine was required, suggesting improved sensitivity with BPEI. The improved ability of BPEI to trigger the aggregation of GNPs could be attributed to the multiple amino groups in a branched molecular structure and larger molecular size of BPEI. On the LF strips, since there was very limited solution in the nitrocellulose membrane, a stronger capability to trigger the aggregation of GNPs allows fewer BPEI molecules to be released from the liposome conjugated to the target bacteria to induce an observable color signal due to the cross-linking of GNPs, suggesting better sensitivity with BPEI rather than L-cysteine.

In ELISA, the capture of target, the labeling of probes and liposome as well as the color change due to GNP aggregation were performed in separate steps with a washing step interval. In contract, in LFIA the same process would have to be performed on the LF strip sequentially. Thus, in the pLFS detection the timing of the addition of probes, streptavidin linker, liposomes and GNPs/PBST mixture is very important for appropriate generation of colorimetric signal. Different detection procedures were investigated to achieve optimal performance. In Fig. 2, various detection procedures were illustrated along with the corresponding results. It was noted that in Procedure A when the probes, streptavidin and liposomes are directly mixed with the sample, there was an observable red dot with the blank, which could be attributed to the cross-linking of the probe-liposome structures trapped in

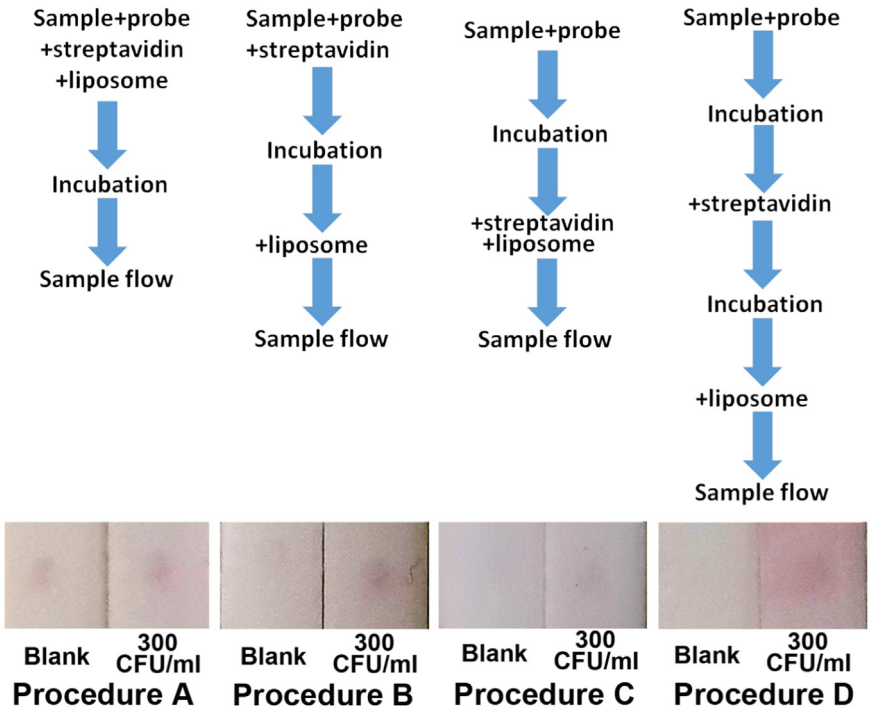

Fig. 2. Schematic of sample preparation steps and representative results (photos) in pLFS experiments from blank samples for *E. coli* O157:H7 concentration of 300 CFU/ml.

the detection zone giving rise to the signal in the following colorimetric generation process. The resulting signal from the blank could be recognized as false positives to influence the reliability of the detection method. Procedures B, C, and D exhibited a clear strip with blank samples, hence false positive was not a concern. These clear strips from blank samples also suggested that the possible cross-linked probes would not induce false positives without liposome. In our evaluation, Procedure C gave the weakest positive signal, suggesting the least sensitivity. Compared with Procedure B, in Procedure C there were more unreacted streptavidin linkers when liposomes were added to induce more liposome network structures. But no obvious spot was noted in Procedure C, suggesting that the cross-linked liposome network structures would not result in false positives which could be attributed to the low concentration of liposomes (1.73×10^{11} liposomes/ml). The weaker signal in Procedure C with *E. coli* O157:H7 compared to that in Procedure B implied that the formed cross-linked liposome network structures would reduce the number of liposomes linked to the probes labeling the captured *E. coli* O157:H7 in the detection zone resulting in low sensitivity. The strongest signal was obtained from Procedure D, however the most complex operation and longer process limited the simplicity and practicality of pLFS, further the intense color in the region around the dot in the detection zone made it hard to recognize the spot from the rest of the area. The difference in results obtained above in the listed procedures indicated that the cross-linked probe-liposome structures should be the main reason for false positives in pLFS. Upon evaluation, Procedure B was chosen as the optimized protocol for the pLFS in the following experiments.

In the pLFS procedure, detection results could be affected by the amount of probes and streptavidin linker incubated with target bacteria in the solution. Meanwhile the antibody immobilized on the LF strip could also influence detection sensitivity. To investigate these factors for the pLFS methodology, serial optimizations were performed. Fig. 3 shows images of the LF strips obtained from pLFS performed under different conditions. It can be seen that when the added GNP probes increased to 10 μl, the obtained signal from a 300 CFU/ml of *E. coli* O157:H7 sample became more intense while a blank signal was noticeable. The reason for an increase in signal strength at 300 CFU/ml of

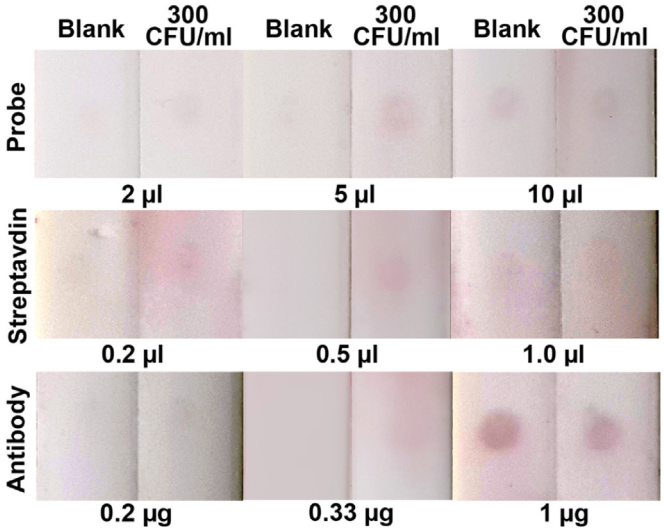

Fig. 3. Photos of LF strip with blank sample (control) and 300 CFU/ml of *E. coli* O157:H7 from pLFS performed under different experimental conditions.

E. coli O157:H7 is due to the increased amount of probes on the target bacteria; however, at higher concentrations, the probes may increase the amount of cross-linked probe-liposome structures trapped in the detection zone to give rise to false positives. It should be noted that the increase in streptavidin did not significantly improve the signals from bacteria compared with blank samples. The attributed reasons are: higher concentration of streptavidin could increase the possibility to cross-link probes and liposomes; however, since the streptavidin (1.8 μM) was present at a much higher concentration than the probes (0.17 nM) and liposomes (1.73×10^{11} liposomes/ml), the change in the concentration of streptavidin would not be a key factor to the formation of cross-linked probe-liposome structures. Based on the results in optimization of detection procedure and conditions, we hypothesized that the cross-linked probe-liposome structures should be the main reason

for false positive signals. The excess streptavidin did not contribute to any significant improvement in the signal from the sample with 300 CFU/ml of *E. coli* O157:H7. The amount of antibody conjugated on the LF strip could affect the results of pLFS. It can be seen that with 1 μg of antibody an intense spot was observed with blank samples though the signals from 300 CFU/ml of *E. coli* O157:H7 was better than the others, indicating that the density of antibodies in the detection zone should be a key factor in the concentration of trapped probe-liposome cross-linked structures which could result in false positives with blank samples. Meanwhile higher concentration of antibodies immobilized on the strip was found to increase the signal at 300 CFU/ml of *E. coli* O157:H7. However, when the amount of antibody immobilized on the LF strip was reduced to 0.2 μg, no signal was observed with the blank sample or 300 CFU/ml of *E. coli* O157:H7, which could be attributed to a lower amount of labeled target bacteria captured at the detection zone. According to the results shown in Fig. 3, the cross-linked probe-liposome structures should be the main reason for false positives, while the amount of probes and antibodies immobilized on the LF strip could affect the detection results more than that of the added streptavidin and liposome.

To demonstrate plasmonic enhancement of the proposed pLFS, serial concentrations of *E. coli* O157:H7 from 100 to 600 CFU/ml were evaluated based on the optimized protocol. Images of the final results from pLFS was illustrated in Fig. 4. To further illustrate the detection performance of pLFS, a comparison was made with conventional LFIA to detect *E. coli* O157:H7 under same condition. It can be seen that with the developed pLFS as low as 100 CFU/ml of bacteria could be recognized with naked eye. However, with conventional LFIA, no visible signal could be observed even at 30,000 CFU/ml of bacteria. Compared to the sensitivity of 10^5–10^6 CFU/ml with conventional LFIA for whole bacterium cells which means the capability to differentiate the concentration change in 10^5 CFU/ml, the recognition of 100 CFU/ml bacteria with pLFS indicates a higher detection accuracy. The comparison demonstrated a dramatically improved sensitivity from pLFS than the conventional LFIA performed under the same conditions. In contrast, the sensitivity of the reported LFIA with silver enhanced LFIA was increased by only 10 times (Wiederoder et al., 2017), while by utilizing the probes fabricated with hierarchical gold nanoparticles, Zhang et al. (2015) achieved a detection sensitivity down to 10^3 CFU/ml with tipped flowerlike GNPs. It can be noted that based on the color from multiple GNPs in the aggregates, the sensitivity of pLFS can be further improved compared to the LFIA with the color from GNP-based probe itself. The pLFS was comparable to the enzyme amplified LFIA which was shown to detect as low as 100 CFU/ml of bacteria (Cho and Irudayaraj, 2013b). A key advantage of pLFS is that the enhancement strategy does not depend on enzymes for color generation and hence has immense practical appeal. It should also be noted from the images, that an increased intensity of red color from pLFS is proportional to the concentration of *E. coli* O157:H7, suggesting its potential in quantitation.

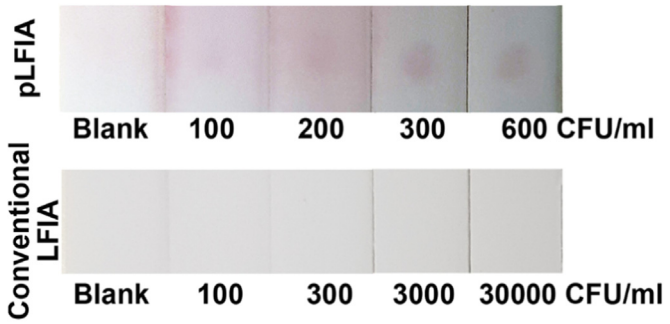

Fig. 4. Comparison between pLFS and conventional LFIA response to serial concentration of *E. coli* O157:H7.

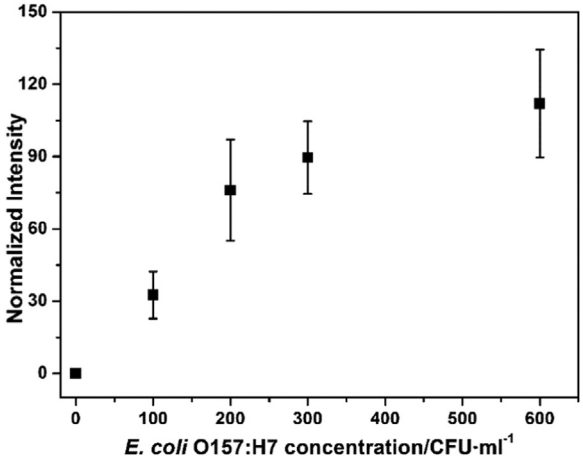

Fig. 5. Quantitative response of the colorimetric signal from pLFS when exposed to *E. coli* O157:H7 at different concentration [mean ± SD, n = 3].

To quantify the response of pLFS, the results based on the intensity of the spots from the samples at a serial concentration of *E. coli* O157:H7 is plotted (Fig. 5). The normalized intensity of the red spots was calculated based on the gray scale value of the spots in the images relative to the results from blank samples as the baseline. It can be seen that the normalized intensity of the dots increased with the concentration of target bacteria. It was also noted that the percent increase in color intensity for concentration range from 300 CFU/ml to 600 CFU/ml was not as much as that from 0 to 300 CFU/ml, which could be attributed to the number of GNP aggregate formation limited by the amount of GNP monomers possibly confined by the pores of the nitrocellulose membrane in the LF strip. To assess the reproducibility of pLFS, the p-value of the quantitative results was evaluated. The p-value between blank and 100 CFU/ml is less than 0.01, indicating a significant difference between the detection results from blank and 100 CFU/ml samples. The p-value between 100 and 200 CFU is 0.053 and the p-value between 200 and 300 CFU/ml is 0.052. The p-values were slightly greater than 0.05 but in the acceptable range mainly due to the heterogeneous distribution of bacteria cells in the 100 μl volume of sample tested in pLFS. As discussed above, the signal from 600 CFU/ml was limited by the amount of GNPs confined in the pores of LF strip, therefore the p-value between 300 and 600 CFU/ml is 0.33. The recovery rate of detection was calculated and shown in Table S1. It can be noted that the recovery rate for 100 CFU/ml sample is only 85.0%, which should be attributed to the low capture efficiency when low concentration of bacteria was tested.

To investigate the detection performance of the proposed pLFS in food samples, cranberry juice obtained from a local market was inoculated with *E. coli* O157:H7 and used in experiments. Since the pH of the packaged juice was around 4 which could potentially influence the antibody capture and probe label, the pH was adjusted to 7 with 1 M NaOH. To reduce the influence from thickening agents in the juice, the juice was diluted with 10 mM PBS in 1:1 ratio. The quantified detection results from pLFS were shown in Fig. 6 and the inset in Fig. 6 shows the image of the strip after experimentation. It can be seen that compared with the results from the bacteria in PBS, the blank juice gave a slight background signal as expected due to interference from the food matrix. Likewise, the quantified signal from 600 CFU/ml in juice (Fig. 6) was weaker than that in PBS (Fig. 5). Although in the inset in Fig. 6, the color signal from 600 CFU/ml of *E. coli* O157:H7 in juice was weaker than the one from PBS (Fig. 4) and a red dot can still be recognized, indicating the potential of the proposed pLFS in food sample monitoring.

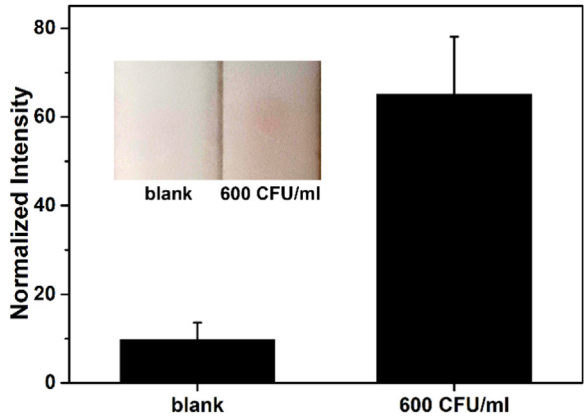

Fig. 6. The quantitative response from blank and 600 CFU/ml of *E. coli* O157:H7 in 1:1 ratio diluted cranberry juice [mean ± SD, n = 3]. Inset is representative image from detection results in cranberry juice.

4. Conclusion

The plasmonic enhancement concept was developed and implemented in an LFIA device utilizing BPEI-loaded liposomes to trigger the aggregation on GNPs for signal generation. The detection procedure complies with the simplicity of the conventional LFIA systems in the market. With the plasmonic enhancement strategy, the detection sensitivity of the pLFS was greatly enhanced rather than that based on the color of probes themselves. The detection procedure and conditions were investigated to achieve optimized performance to detect as low as 100 CFU/ml of *E. coli* O157:H7, which is 1000 folds better than the conventional LFIA platforms and comparable to the enzyme amplified LFIA. Meanwhile with pLFS, 600 CFU/ml of *E. coli* O157:H7 can be recognized with naked eyes in juice samples. The pLFS concept developed does not require enzymes for color generation or enhancement and thus eliminates issues related to enzyme stability and bioactivity inherent to enzyme-based colorimetric reaction. Results indicate that the proposed pLFS exhibits a strong potential for detecting various bacteria targets. Meanwhile by loading different chemicals in the liposome, the pLFS platform could provide the flexibility for signal enhancement to detect multiple targets.

Acknowledgement

This research is supported by the U.S. Department of Agriculture, Agricultural Research Service, under Project No. 59-8072-6-001. Any opinions, findings, conclusion, or recommendations expressed in this publication are those of the author(s) and do not necessarily reflect the view of the U.S. Department of Agriculture.

Appendix A. Supporting information

Supplementary data associated with this article can be found in the online version at doi:10.1016/j.bios.2018.10.066.

References

Bui, M.-P.N., Ahmed, S., Abbas, A., 2015. Single-digit pathogen and attomolar detection with the naked eye using liposome-amplified plasmonic immunoassay. Nano Lett. 15 (9), 6239–6246.
Chen, H.D., Frankel, G., 2005. Enteropathogenic *Escherichia coli*: unravelling pathogenesis. FEMS Microbiol. Rev. 29 (1), 83–98.
Cho, I.-H., Irudayaraj, J., 2013a. In-situ immuno-gold nanoparticle network ELISA biosensors for pathogen detection. Int. J. Food Microbiol. 164 (1), 70–75.
Cho, I.-H., Irudayaraj, J., 2013b. Lateral-flow enzyme immunoconcentration for rapid detection of Listeria monocytogenes. Anal. Bioanal. Chem. 405 (10), 3313–3319.
Corstjens, P., Zuiderwijk, M., Nilsson, M., Feindt, H., Niedbala, R.S., Tanke, H.J., 2003. Lateral-flow and up-converting phosphor reporters to detect single-stranded nucleic acids in a sandwich-hybridization assay. Anal. Biochem. 312 (2), 191–200.
Cox, C.R., Jensen, K.R., Mondesire, R.R., Voorhees, K.J., 2015. Rapid detection of Bacillus anthracis by γ phage amplification and lateral flow immunochromatography. J. Microbiol. Methods 118, 51–56.
De La Rica, R., Stevens, M.M., 2012. Plasmonic ELISA for the ultrasensitive detection of disease biomarkers with the naked eye. Nat. Nanotechnol. 7 (12), 821.
De La Rica, R., Stevens, M.M., 2013. Plasmonic ELISA for the detection of analytes at ultralow concentrations with the naked eye. Nat. Protoc. 8 (9), 1759.
Doremus, R.H., 1964. Optical properties of small gold particles. J. Chem. Phys. 40 (8), 2389–2396.
Famewo, E.B., Clarke, A.M., Afolayan, A.J., 2016. Identification of bacterial contaminants in polyherbal medicines used for the treatment of tuberculosis in Amatole District of the Eastern Cape Province, South Africa, using rapid 16S rRNA technique. J. Health Popul. Nutr. 35 (1), 27.
Frens, G., 1973. Controlled nucleation for regulation of particle-size in monodisperse gold suspensions. Nat.-Phys. Sci. 241 (105), 20–22.
Gobbo, P., Biondi, M.J., Feld, J.J., Workentin, M.S., 2013. Arresting the time-dependent H 2 O 2 mediated synthesis of gold nanoparticles for analytical detection and preparative chemistry. J. Mater. Chem. B 1 (33), 4048–4051.
Gomes, J.F.Pd.S., Sonnen, A.F.-P., Kronenberger, A., Fritz, J., Coelho, M.Á.N., Fournier, D., Fournier-Nöel, C., Mauzac, M., Winterhalter, M., 2006. Stable polymethacrylate nanocapsules from ultraviolet light-induced template radical polymerization of unilamellar liposomes. Langmuir 22 (18), 7755–7759.
Gumustas, A., Caglayan, M.G., Eryilmaz, M., Suludere, Z., Soykut, E.A., Uslu, B., Boyaci, I.H., Tamer, U., 2018. Paper based lateral flow immunoassay for the enumeration of *Escherichia coli* in urine. Anal. Method. 10 (10), 1213–1218.
Guo, S., Wang, E., 2011. Noble metal nanomaterials: controllable synthesis and application in fuel cells and analytical sensors. Nano Today 6 (3), 240–264.
Haiss, W., Thanh, N.T., Aveyard, J., Fernig, D.G., 2007. Determination of size and concentration of gold nanoparticles from UV− Vis spectra. Anal. Chem. 79 (11), 4215–4221.
Hua, F., Zhang, P.P., Zhang, F.L., Zhao, Y., Li, C.F., Sun, C.Y., Wang, X.C., Yang, R.F., Wang, C.B., Yu, A.L., Zhou, L., 2015. Development and evaluation of an up-converting phosphor technology-based lateral flow assay for rapid detection of Francisella tularensis. Sci. Rep. 5, 17178.
Imamura, K., Takayama, S., Saito, A., Inoue, E., Nakayama, Y., Ogata, Y., Shirakawa, S., Nagano, T., Gomi, K., Morozumi, T., 2015. Evaluation of a novel immunochromatographic device for rapid and accurate clinical detection of Porphyromonas gingivalis in subgingival plaque. J. Microbiol. Methods 117, 4–10.
Lee, S., Mehta, S., Erickson, D., 2016. Two-color lateral flow assay for multiplex detection of causative agents behind acute febrile illnesses. Anal. Chem. 88 (17), 8359–8363.
Li, Z.H., Wang, Y., Wang, J., Tang, Z.W., Pounds, J.G., Lin, Y.H., 2010. Rapid and sensitive detection of protein biomarker using a portable fluorescence biosensor based on quantum dots and a lateral flow test strip. Anal. Chem. 82 (16), 7008–7014.
Linares, E.M., Kubota, L.T., Michaelis, J., Thalhammer, S., 2012. Enhancement of the detection limit for lateral flow immunoassays: evaluation and comparison of bioconjugates. J. Immunol. Methods 375 (1–2), 264–270.
Liu, J.W., Mazumdar, D., Lu, Y., 2006. A simple and sensitive “dipstick” test in serum based on lateral flow separation of aptamer-linked nanostructures". Angew. Chem. Int. Ed. Engl. 45 (47), 7955–7959.
Luo, K., Hu, L.M., Guo, Q., Wu, C.H., Wu, S.S., Liu, D.F., Xiong, Y.H., Lai, W.H., 2017. Comparison of 4 label-based immunochromatographic assays for the detection of *Escherichia coli* O157:H7 in milk. J. Dairy Sci. 100 (7), 5176–5187.
Mao, X., Ma, Y.Q., Zhang, A.G., Zhang, L.R., Zeng, L.W., Liu, G.D., 2009. Disposable nucleic acid biosensors based on gold nanoparticle probes and lateral flow strip. Anal. Chem. 81 (4), 1660–1668.
Nie, X.-M., Huang, R., Dong, C.-X., Tang, L.-J., Gui, R., Jiang, J.-H., 2014. Plasmonic ELISA for the ultrasensitive detection of Treponema pallidum. Biosens. Bioelectron. 58, 314–319.
Panferov, V.G., Safenkova, I.V., Varitsev, Y.A., Drenova, N.V., Kornev, K.P., Zherdev, A.V., Dzantiev, B.B., 2016. Development of the sensitive lateral flow immunoassay with silver enhancement for the detection of Ralstonia solanacearum in potato tubers. Talanta 152, 521–530.
Pappert, G., Rieger, M., Niessner, R., Seidel, M., 2010. Immunomagnetic nanoparticle-based sandwich chemiluminescence-ELISA for the enrichment and quantification of *E. coli*. Microchim. Acta 168 (1–2), 1–8.
Pengsuk, C., Chaivisuthangkura, P., Longyant, S., Sithigorngul, P., 2013. Development and evaluation of a highly sensitive immunochromatographic strip test using gold nanoparticle for direct detection of Vibrio cholerae O139 in seafood samples. Biosens. Bioelectron. 42, 229–235.
Preechakasedkit, P., Pinwattana, K., Dungchai, W., Siangproh, W., Chaicumpa, W., Tongtawe, P., Chailapakul, O., 2012. Development of a one-step immunochromatographic strip test using gold nanoparticles for the rapid detection of Salmonella typhi in human serum. Biosens. Bioelectron. 31 (1), 562–566.
Rajendran, V.K., Bakthavathsalam, P., Ali, B.M.J., 2014. Smartphone based bacterial detection using biofunctionalized fluorescent nanoparticles. Microchim. Acta 181 (15–16), 1815–1821.
Ren, W., Cho, I.-H., Zhou, Z., Irudayaraj, J., 2016. Ultrasensitive detection of microbial cells using magnetic focus enhanced lateral flow sensors. Chem. Commun. 52 (27), 4930–4933.
Ren, W., Liu, W., Irudayaraj, J., 2017. A net fishing enrichment strategy for colorimetric detection of *E. coli* O157: H7. Sens Actuator B-Chem. 247, 923–929.
Ren, W., Wang, R., Ouyang, L., Irudayaraj, I., 2018. New developments in detection technologies for Escherichia coli and other pathogenic organisms. In: Fratamico, P.M., Liu, Y., Sommers, C.H. (Eds.), Pathogenic *Escherichia coli*: Evolution, Omics, Detection and Control. Caister Academic Press, Wyndmoor, USA, pp. 85–107.
Shin, J.H., Hong, J., Go, H., Park, J., Kong, M., Ryu, S., Kim, K.P., Roh, E., Park, J.K.,

2018. Multiplexed detection of foodborne pathogens from contaminated lettuces using a handheld multistep lateral flow assay device. J. Agric. Food Chem. 66 (1), 290–297.
Song, C., Liu, J., Li, J., Liu, Q., 2016. Dual FITC lateral flow immunoassay for sensitive detection of *Escherichia coli* O157:H7 in food samples. Biosens. Bioelectron. 85, 734–739.
Song, L., Zhang, L., Huang, Y., Chen, L., Zhang, G., Shen, Z., Zhang, J., Xiao, Z., Chen, T., 2017. Amplifying the signal of localized surface plasmon resonance sensing for the sensitive detection of *Escherichia coli* O157:H7. Sci. Rep. 7 (1), 3288.
Wiederoder, M., Smith, S., Madzivhandila, P., Mager, D., Moodley, K., DeVoe, D., Land, K., 2017. Novel functionalities of hybrid paper-polymer centrifugal devices for assay performance enhancement. Biomicrofluidics 11 (5), 054101.
Xing, K.Y., Peng, J., Liu, D.F., Hu, L.M., Wang, C., Li, G.Q., Zhang, G.G., Huang, Z., Cheng, S., Zhu, F.F., Liu, N.M., Lai, W.H., 2018. Novel immunochromatographic assay based on Eu (III)-doped polystyrene nanoparticle-linker-monoclonal antibody for sensitive detection of *Escherichia coli* O157:H7. Anal. Chim. Acta 998, 52–59.
Xu, Q., Xu, H., Gu, H., Li, J., Wang, Y., Wei, M., 2009. Development of lateral flow immunoassay system based on superparamagnetic nanobeads as labels for rapid quantitative detection of cardiac troponin I. Mater. Sci. Eng., C. 29 (3), 702–707.
Zhang, L., Huang, Y., Wang, J., Rong, Y., Lai, W., Zhang, J., Chen, T., 2015. Hierarchical flowerlike gold nanoparticles labeled immunochromatography test strip for highly sensitive detection of *Escherichia coli* O157:H7. Langmuir 31 (19), 5537–5544.